PERKIN 2

Complexes of the $H_5O_2^+$ and H_3O^+ cations with polyethers in water saturated dichloroethane solutions. A combined IR spectroscopic and quantum mechanics study †

A. Varnek,[a] G. Wipff,*[a] A. Famulari,[b] M. Raimondi,[b] T. Vorob'eva[c] and E. Stoyanov[c]

[a] Laboratoire MSM, UMR 7551 CNRS, 4, rue Strasbourg, 67000, France
[b] Department of Physical Chemistry and Electrochemistry, University of Milan, via Goldi 19, Milan, Italy
[c] Institute of Catalysis, Russian Academy of Sciences, av. Lavrentiev, 5, Novosibirsk, Russia

Received (in Cambridge, UK) 28th January 2002, Accepted 8th March 2002

We report combined IR spectroscopic and quantum mechanical studies on the interactions between hydrated proton (H_3O^+ and $H_5O_2^+$) and polyethers (**L** = 15-crown-5, 18-crown-6, benzo-18-crown-6 and polyethylene glycols PEG-400 and PEG-600) in 1,2-dichloroethane (DCE) solution saturated with water, in the presence of non-coordinating chlorinated cobalt dicarbollide anions. The state of the hydrated proton and composition of the complexes are shown to depend on the nature and concentration of the ligand. Thus, 15-crown-5 forms $[H_3O^+\cdot\mathbf{L}]$ and $[H_5O_2^+\cdot 2\mathbf{L}]$ complexes at small and high concentrations of **L**, respectively. At all studied concentrations, 18-crown-6 and benzo-18-crown-6 form only $[H_3O^+\cdot\mathbf{L}]$ type complexes, whereas PEGs form 1 : 1 complexes with $H_5O_2^+$. The coordination patterns of the hydrated proton depend on the topology, flexibility/rigidity and the number of donor centres of **L**. In the $[H_3O^+\cdot(18c6)]$, $[H_3O^+\cdot(B18c6)]$ and $[H_5O_2^+\cdot 2(15c5)]$ complexes, the hydrated proton forms preferentially O–H ··· O_L linear hydrogen bonds. In $[H_3O^+\cdot 15c5]$, H_3O^+ interacts with all 5 O-atoms of 15c5 *via* one linear and two asymmetric bifurcated H-bonds. We also report the first IR characterization of the $[H_5O_2^+\cdot 4H_2O]$ cation complex in an organic solution.

1 Introduction

The extraction of metals by polyethers (**L**) from acidic media to an organic phase is usually accompanied by the complexation of **L** by the hydrated proton $H(H_2O)_n^+$ whose nature (generally H_3O^+ or $H_5O_2^+$) depends on **L**. Thus, stable complexes of cyclic 18-crown-6 with H_3O^+ have been characterized in the gas phase,[1] in various solutions and in the solid state,[2,3] whereas macrocycles with larger cavities such as 21-crown-7,[4] 2-sulfo-1,3-xylyl-21-crown-7 and 2-sulfo-1,3-xylyl-27-crown-9[5] bind $H_5O_2^+$. Complexes of the hydrated proton with polyethylene glycols (PEG) have not been so far characterized in the solid state because of crystallisation problems.

The type of complex formed by the hydrated proton generally critically depends on the nature and concentration of **L** and counter-ions, and on the water content. IR spectroscopy studies[6–10] show that, in weakly polar solvents, interactions of the hydrated proton with the O_L oxygen atom of *monodentate* ligands containing a phosphoryl, carbonyl or ether group, lead to the formation of $H_3O^+\cdot 3O_L$, $H_5O_2^+\cdot 4O_L$ or $H_5O_2^+\cdot nH_2O\cdot mO_L$ sub-structures. For *polydentate* ligands like crown-ethers and their open-chain analogues one may expect co-operative hydrogen bonds between the hydrated proton and several oxygen atoms of **L** or between one O_L oxygen and two oxonium protons.

Several structures of complexes of the hydrated proton with crown-ethers in the solid state are available in the Cambridge Crystallographic Database[11,12] and have been reported in a review paper,[2] but details of hydrogen bonding patterns are often lacking due to difficulties in localising hydrogen atoms in X-ray diffraction experiments. They show that the precise position of the oxygen atom of H_3O^+ with respect to the crown may depend on the counter-ion and packing effects. It is however unclear whether these structures are representative of those present in weakly polar solvents (dichloroethane, chloroform, *etc.*) saturated with water.

This led us to investigate by IR spectroscopy the nature of the complexes between the hydrated proton and polyether ligands **L** in an organic solution saturated with water. As ligands, we compared 15-crown-5 (15c5), 18-crown-6 (18c6), benzo-18-crown-6 (B18c6) and polyethylene glycols PEG-400 and PEG-600 (Chart 1). PEG-400 and PEG-600 contain mixtures of linear $HO–CH_2–(CH_2–O–CH_2)_m–CH_2–OH$ molecules corresponding to average molecular masses of 400 and 600 a.u., respectively. The $H^+\cdot nH_2O\cdot\mathbf{L}$ complexes were investigated in water saturated solutions of 1,2-dichloroethane (DCE) with chlorinated cobalt dicarbollide $[Co(C_2B_9H_8Cl_3)_2^-]$ (**CCD**$^-$; see Chart 1) as counterion. This hydrophobic bulky anion, as a non-coordinating species, should not perturb the coordination patterns of the $H^+\cdot nH_2O\cdot\mathbf{L}$ complexes. Comparison of the different polyethers gives insights into the state of the hydrated proton as a function of the topology of **L** (macrocyclic *vs.* open-chain ligands), of the ring size (15c5 *vs.* 18c6) and of the substituent effects (18c6 *vs.* B18c6). The information inferred from IR data is used to modelbuild the corresponding H_3O^+ or $H_5O_2^+$ complexes "in the gas phase", using quantum mechanical approaches, thus leading to microscopic insights into the hydrogen binding patterns between the hydrated proton and the different polyethers.

2 Experimental

2.1 Spectroscopy studies

2.1.1 Reagents and apparatus. 1,2 Dichloroethane (DCE) of chemical purity grade was purified using standard methods.

---

† Electronic supplementary information (ESI) available: the coordinates of the 6-31G* optimized systems (four files in PDB format). See http://www.rsc.org/suppdata/p2/b2/b201034h/

DOI: 10.1039/b201034h

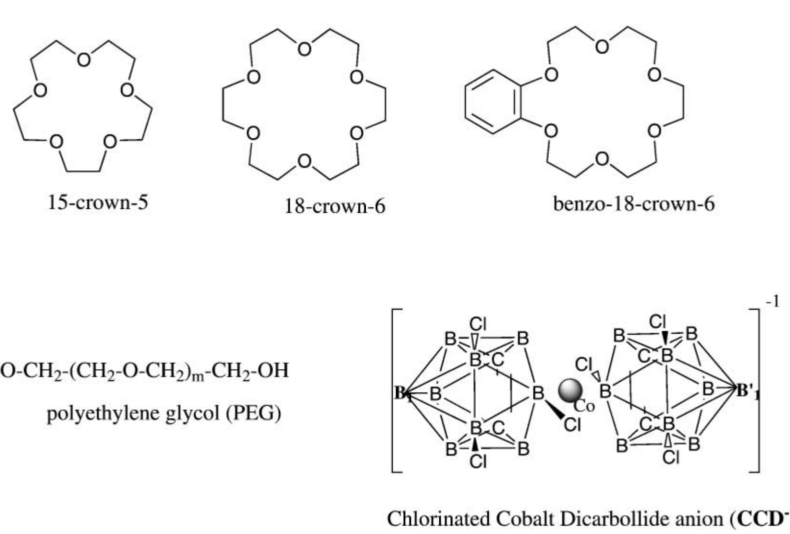

Chart 1 Studied polyethers and chlorinated cobalt dicarbollide anion used in experiments. The average number ***m*** of $–CH_2–O–CH_2–$ of polyethylene glycols is 8 for PEG-400 and 12 for PEG-600.

Chlorinated cobalt dicarbollide $\mathbf{CCD}^-$ (90% in H-form and 10% in Na-form) from KATCHEM Co. (Czech Republic), 15c5 and 18c6 from REAKTIV-SERVIS (Moscow, Russia), and polyethylene glycols PEG-400 and PEG-600 from VEKTON (St. Petersburg, Russia) were used without any additional purification. $\mathbf{CCD}^-$ was preliminarily converted into 100% H-form by mixing its DCE solution with 3 M H_2SO_4 aqueous solution for 5 min. Dry dichloroethane solutions of H**CCD** + polyethers were prepared by mixing DCE solutions of H**CCD** and of polyethers, prepared by dissolving weighed amounts of H**CCD** or polyether. The resulting solutions were then equilibrated with water.

IR spectra were recorded on a BOMEM M-102 FTIR spectrometer (40 scans, resolution 4 cm^{-1}) in the 920–4000 cm^{-1} range using cells with BaF_2 windows. ^1H NMR spectra were registered on a DPX-250 spectrometer (Bruker). The signals at 4.81, 4.76, 4.71 and 4.55 ppm of $\mathbf{CCD}^-$ were used as an internal standard. The concentration of water in DCE solutions was determined by comparing its integrated intensity with that of $\mathbf{CCD}^-$.

2.1.2 Separation of the IR spectra of proton hydrates from the IR spectra of solutions. The IR absorption spectra (denoted by $\boldsymbol{S}$) of water saturated DCE solutions result from overlapping contributions of the solvent ($\boldsymbol{S}_{DCE}$), dissolved water ($\boldsymbol{S}_{wat}$) and the hydrated proton complexes **X** ($\boldsymbol{S}_X$). In order to extract the $\boldsymbol{S}_X$ bands from the spectrum $\boldsymbol{S}$ of a given solution, we subtracted the $\boldsymbol{S}_i$ bands of individual components (i = DCE, H_2O, **L**): $\boldsymbol{S}_X = \boldsymbol{S} - \Sigma(f_i{\cdot}\boldsymbol{S}_i)$, where f_i are scaling factors. Subtraction of $\boldsymbol{S}_L$ from $\boldsymbol{S}$ removes the contribution of uncomplexed **L** and, in particular, of the corresponding $\nu_{as}(COC)$ band.

Two different types of water molecules, denoted by $\boldsymbol{S}_{wat1}$ and $\boldsymbol{S}_{wat2}$, were found in the spectra of the "humid" DCE solutions. $\boldsymbol{S}_{wat1}$ with the bands at 3775, 3593 cm^{-1} and 1607 cm^{-1} represents "isolated" H_2O molecules (not involved in hydrogen bonds with the solute), whose concentration is equal to the solubility of water in DCE (0.1 mol l^{-1}). $\boldsymbol{S}_{wat2}$ corresponds to self-associated water ("extra" water) with typical stretching $\nu(H_2O) \approx 3400$ cm^{-1} and bending $\delta(H_2O) = 1637–1640$ cm^{-1} vibrations (Figs. 1 and 2), whose intensities depend on the composition of the studied solution and on the way it was prepared.

Two different methods were used to isolate the $\boldsymbol{S}_{wat2}$ spectrum. The first one is based on the decrease of the total water content when the concentrations of the proton complex **X** or of $H^+\mathbf{CCD}^-$ increase. Fig. 1 presents an example of obtaining $\boldsymbol{S}_{wat2}$ from the difference between two spectra of 0.071 M and 0.1 M H^+**CCD** solutions in DCE. Fitting the scaling factor allowed removal of the $H^+\mathbf{CCD}^-$ bands in the residual spectrum, which thus contains the bands of "extra" water only (Fig. 1c). For solutions containing polyethers and their complexes, the $\boldsymbol{S}_{wat2}$ bands were obtained analogously.

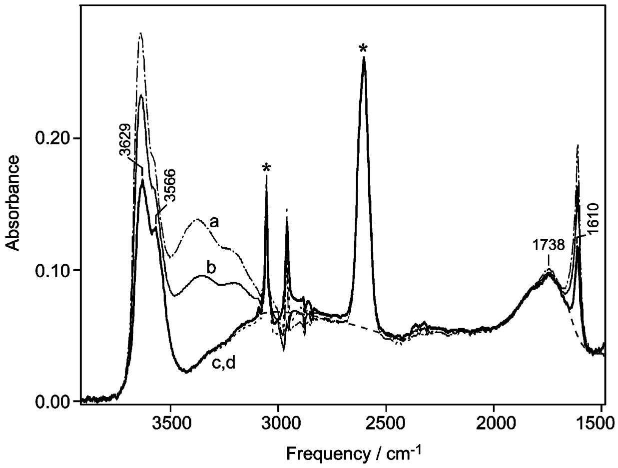

Fig. 1 IR spectra of water saturated DCE solutions of 0.071 M (***a***) and 0.1 M (***b***) $H^+\mathbf{CCD}^-$. Spectra (***c***) and (***d***) of the $H_5O_2^+{\cdot}4H_2O$ cation were obtained by subtracting the spectrum of "excess" water from (***a***) and (***b***), respectively. All spectra were normalized to 0.1 M concentration. The bands ν(CH) and ν(BH) of $\mathbf{CCD}^-$ are marked by (*).

The second method is based on the comparison of solutions obtained by two different protocols (***a*** and ***b***, respectively; see Fig. 2). The solution ***a*** is prepared by mixing equal volumes of the water saturated solutions of $H^+\mathbf{CCD}^-$ and of **L** in DCE. The mixture becomes turbid due to formation of water droplets which are expelled from the solution by centrifugation. Solution ***b*** is prepared by shaking solution ***a*** with distilled water for 5 min. The intensities of isolated water molecules band $\boldsymbol{S}_{wat1}$ at 3775 and 3593 cm^{-1} in ***a*** and ***b*** are similar, while the intensities of the $\boldsymbol{S}_{wat2}$ bands in ***b*** are larger than in ***a***. Thus, the spectrum of "extra water" $\boldsymbol{S}_{wat2}$ can be obtained as a difference of the spectra of ***a*** and ***b*** (Fig. 2).

Finally, the IR spectrum of a given proton complex **X** is calculated as $\boldsymbol{S}_X = \boldsymbol{S} - f_{DCE}{\cdot}\boldsymbol{S}_{DCE} - f_L{\cdot}\boldsymbol{S}_L - f_{wat2}{\cdot}\boldsymbol{S}_{wat2}$. The scaling factor f_L of $\boldsymbol{S}_L$ was used to calculate the concentration of complexed **L** in extracts: $C_{compl} = C_0 - f_L{\cdot}C_{st}$, where C_0 is the total concentration of **L** in solution, and C_{st} is the concentration of **L** in standard solution for which the $\boldsymbol{S}_L$ spectrum was recorded. The stoichiometry of the complexes was inferred from the C_{compl}/C_{HCCD} ratio.

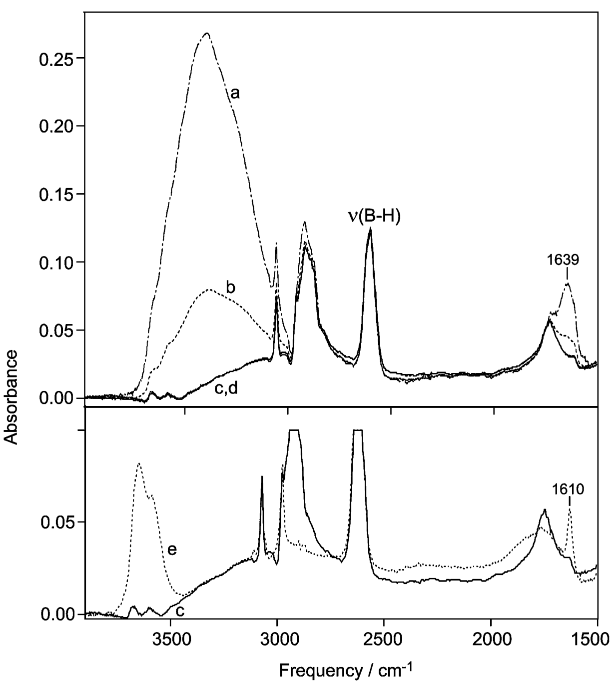

Fig. 2 IR spectra of wet DCE solutions of 0.05 M H^+**CCD**$^-$ + 0.05 M PEG-400. Solutions were obtained: (***a***) by mixing calculated volumes of water-saturated solutions H^+**CCD**$^-$ and PEG-400; (***b***) after additional mixing of the solution *a* with water for 5 min. The spectra (***c***) and (***d***) of the $H_5O_2^+$·PEG complex were obtained by subtracting the spectrum of "excess" water from (***a***) and (***b***), respectively. The spectrum of $H_5O_2^+$·$4H_2O$ (***e***) is given for comparison.

2.2 Quantum mechanics calculations

2.2.1 Hartree–Fock calculations. Hartree–Fock (HF) *ab initio* calculations on the free ligands **L** and their complexes with H_3O^+ or $H_5O_2^+$ were performed using the SPARTAN 5.1 program, using the 6-31G* basis set.[13] The structures of the complexes were modelbuilt, using solid state structures of the ligand, when available. They were optimized using first the semi-empirical PM3 method and, subsequently, by *ab initio* quantum mechanical ("QM") calculations. The H_3O^+–**L** interaction energies ($E_{H_3O\cdots L}$) were calculated as $E_{H_3O\cdots L} = E_{H_3O\text{–}L} - (E_{H_3O} + E_L)$, where $E_{H_3O\text{–}L}$, E_{H_3O} and E_L are the total energies of optimized **L**·H_3O^+, H_3O^+ and **L**, respectively. In order to investigate the basis set effects, HF/6-31G** and HF/6-311G** calculations were also performed on the 18c6·H_3O^+ complex. The 6-31G* optimized structures of the 15c5·H_3O^+, 18c6·H_3O^+, benzo-18c6·H_3O^+ and PEG·$H_5O_2^+$ complexes are given as supplementary material.

2.2.2 Valence bond SCF-MI (Self Consistent Field for Molecular Interactions) calculations. Valence bond SCF-MI[14] *ab initio* 6-31G* calculations on the 18c6·H_3O^+ complex were performed using the GAMESS-US suite of programs.[15] The SCF-MI method has been developed for the determination of the intermolecular forces between weakly interacting molecules taking into account the basis set superposition error.[16] Its performance has been tested on large van der Waals molecules, on several combinations of the DNA base pairs and their complexes with H^+, water and some alkali and alkaline-earth cations.[17–21] The initial structures were the same as for Hartree–Fock calculations. A recent review on hydrogen bond calculations with water can be found in ref. 22.

3 Results

3.1 IR spectroscopy characterisation of the hydrated proton species and stoichiometry of the complexes in water saturated DCE solutions

3.1.1 Water saturated H^+CCD$^-$ solutions. The IR spectra of water saturated DCE solutions of H^+**CCD**$^-$ contain a broad band δ(HOH) at 1738 cm^{-1} and an intense continuum broad absorption within 3000–1500 cm^{-1}, which are typical for the cation of [$H_5O_2^+$·4**L**] type, where **L** contains oxygen sites.[6,7,9,10] The spectra also exhibit absorption bands from H_2O molecules bounded with $H_5O_2^+$ and from "extra" water (Fig. 1). The frequency (1632 cm^{-1}) and half-width of the δ(HOH) band of "extra" water are typical for hydrogen-bonded H_2O molecules which do not interact with $H_5O_2^+$.[7]

Having subtracted the "extra" water spectrum from the IR spectra of several [$H_5O_2^+$·$m$$H_2O$]**CCD**$^-$ solutions with different water contents, we obtained identical spectra for the [$H_5O_2^+$·$m$$H_2O$] cations (for example, ***c*** and ***d*** in Fig. 2), which confirms that "extra" water does not interact with the [$H_5O_2^+$·$m$$H_2O$] cation (denoted by **I**). The IR spectrum of **I** contains, in addition to the specific absorption of $H_5O_2^+$,[6–10] the bands at 3629, 3566 and 1610 cm^{-1} of H_2O molecules with free OH groups, coordinated to $H_5O_2^+$ (Fig. 1).

The corresponding number *m* of H_2O molecules was obtained as follows. ^{1}H NMR spectroscopy was used to determine the $H_2O/H_5O_2^+$ ratio (including "extra" water molecules). The total water content was obtained from the molar intensities of δ(HOH) bands at 1610 cm^{-1} in the IR spectra, assuming that they result from all types of H_2O molecules. The number of first shell water molecules is obtained from the intensity of the δ(HOH) band in isolated **I** (spectra ***c*** and ***d*** in Fig. 1). Thus, the calculated value of *m* in the [$H_5O_2^+$·$m$$H_2O$] cation is 4.1, which is close to the expected coordination number 4 for $H_5O_2^+$ (Chart 2).

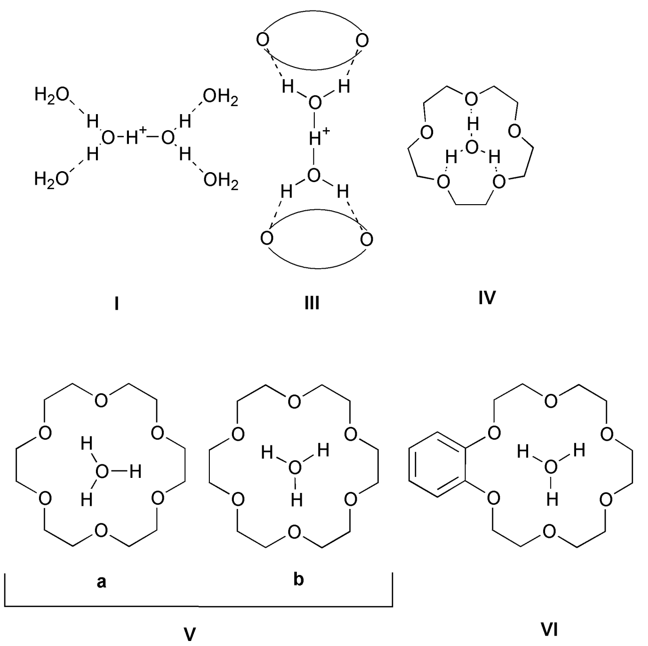

Chart 2 Schematic representation of the $H_5O_2^+$ cation coordinated to four water molecules (**I**) and $H_5O_2^+$·(15-crown-5)$_2$ (**III**). The H_3O^+ complexes with 15-crown-5 (**IV**), 18-crown-6 (**V**) and benzo-18-crown-6 (**VI**). For **V**, two possible orientations of H_3O^+ in the macrocyclic cavity of 18-crown-6, with bifurcated hydrogen bonds (**a**) and with linear hydrogen bonds (**b**), are shown.

3.1.2 H^+CCD$^-$–PEG solutions. The spectra of the complexes formed in 0.05 M H^+**CCD**$^-$ + 0.05 M PEG-400 (or PEG-600) solutions were obtained by subtracting the "extra" water bands from the initial IR spectra of these solutions (Fig. 2, *c* and *d*). They exhibit absorption typical of $H_5O_2^+$ where each of the four hydrogen atoms interacts with an oxygen atom of **L** or of H_2O. Since the spectra contain no absorption bands of H_2O, the $H_5O_2^+$ cation in the $H_5O_2^+$·PEG complex (denoted by **II**) is bound to the oxygen atoms of COC or COH groups of PEG only.

3.1.3 H^+CCD^-–15c5 solutions. The IR spectra of these solutions vary as a function of the molar ratio 15c5 : $H^+\mathbf{CCD}^-$. When this ratio is lower than 1, only the bands of 1 : 1 complexes are developed. As it exceeds 1, new bands of 2 : 1 complexes appear, and their intensity increases up to a maximum when the ratio becomes ≥ 2. These 1 : 1 and 1 : 2 complexes, denoted by **III** and **IV**, respectively, are discussed below.

*1 : 1 complex (**III**).* The IR spectra were recorded for the solution containing 0.1 M $H^+\mathbf{CCD}^-$ + 0.073 M 15c5, where $H^+\mathbf{CCD}^-$ was taken in a small excess in order to shift the 1 : 1 ↔ 1 : 2 equilibrium to the left. The spectrum of **III** was obtained by subtracting the bands of $H^+\mathbf{CCD}^-$ in excess and those of "extra" water from the initial IR spectrum (Fig. 3, *b*).

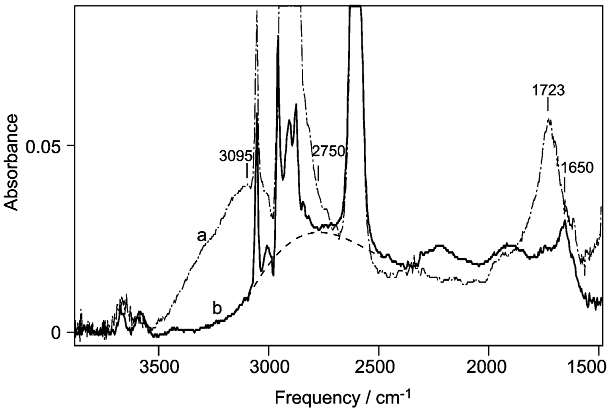

Fig. 3 IR spectra of solutions containing $[H_5O_2^+\cdot(15c5)_2]$ (***a***) and $[H_3O^+\cdot15c5]$ (***b***) species.

It contains the following characteristic features. (i) A broad band of the stretching vibrations of O–H ··· (O_L) groups at ~2750 cm^{-1} that can belong to $H_3O^+\cdot3O_L$ or $H_5O_2^+\cdot4O_L$ cations. (ii) Two weak bands at 1906 and 1650 cm^{-1}, which result from the splitting of the doubly degenerate asymmetric bending vibration ν_4 of H_3O^+, asymmetrically coordinated to 15c5. Note that the $H_5O_2^+\cdot4O_L$ cation always develops one bending vibration in this region (at ~1740 cm^{-1}). (iii) A broad continuum absorption in the whole frequency range below 3200 cm^{-1} which is typical for asymmetric H_3O^+ cations.[6] The complex **III** is thus $[H_3O^+\cdot15c5]$.

*1 : 2 complex (**IV**).* Subtraction of the "extra" water absorption from the IR spectra of the 0.05 M $H^+\mathbf{CCD}^-$ + 0.10 M 15c5 solution leads to the spectrum of the 1 : 2 complex **IV** (Fig. 3, *a*) containing absorption typical of $H_5O_2^+$ whose protons are hydrogen bonded to 15c5. Hence, complex **IV** is $[H_5O_2^+\cdot(15c5)_2]$.

3.1.4 H^+CCD^-–18c6 solutions. Several solutions with the 18c6 : $H^+\mathbf{CCD}^-$ ratio varying from 0.1 to 2 were studied. When this ratio was ≤ 1, the spectra developed a band ν_{as}(COC) = 1095 cm^{-1} corresponding to COC groups of the bonded ligand. Its intensity reached a plateau at 18c6 : $H^+\mathbf{CCD}^-$ ≥ 1. This means that 18c6 forms only a 1 : 1 complex (**V**) with the hydrated proton.

The IR spectrum of the fresh DCE solution of 0.05 M $H^+\mathbf{CCD}^-$ and 0.05 M 18c6 contains low intensity bands of "extra" water (Fig. 4, *a*). Drying this solution over P_2O_5 leads to the disappearance of these bands (Fig. 4, *b*), but does not modify the bands of **V**. ^1H NMR detected five OH protons per ligand in the initial "wet" solution and only three OH protons in the "dry" solution. Hence, the composition of **V** is $H_3O^+\cdot18c6$. The spectrum of **V** agrees with that reported for $H_3O^+\cdot18c6$ in the solid state.[23–25]

3.1.5 H^+CCD^-–benzo-18c6 solutions. In the IR spectra of the $H^+\mathbf{CCD}^-$ + B18c6 solutions the intensity of the ν_{as}(COC) bands of the bonded ligand reaches a plateau at molar ratio $H^+\mathbf{CCD}^-$: B18c6 ≥ 1. These spectra are similar to those of complexes **III** with 18c6, where a continuous broad absorption region within 3300–1400 cm^{-1} indicates an asymmetrical coordination of H_3O^+.[9] Thus, the solutions contain only one type of complex, which is $H_3O^+\cdot$B18c6 (**VI**).

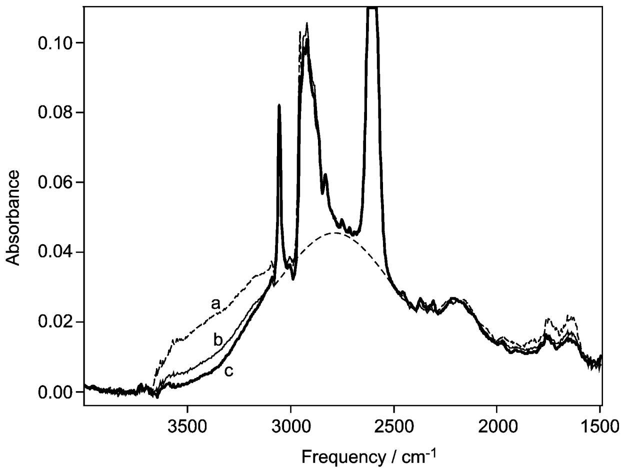

Fig. 4 IR spectra of wet DCE solution of 0.05 M $H^+\mathbf{CCD}^-$ + 0.05 M 18c6: initial solution saturated with water before (***a***) and after (***b***) drying over P_2O_5. (***c***) The spectrum of $H_3O^+\cdot18c6$ obtained by subtracting the spectrum of "excess" water from (***a***) or (***b***).

3.2 Quantum mechanics calculations on the complexes of polyethers with the hydrated proton

In this section we describe the quantum mechanics optimized structures of the H_3O^+ and $H_5O_2^+$ complexes of **L** (**L** = 15c5, 18c6, B18c6 and PEG).

3.2.1 $15c5\cdot H_3O^+$ complex. In the optimized $15c5\cdot H_3O^+$ complex, H_3O^+ forms three short hydrogen bonds with the ligand (Fig. 5). The shortest OH ··· O bond (1.64 Å) is linear, the two others of 1.71 Å are slightly bent (152°). The two other crown oxygens, not formally involved in the hydrogen bonding, are 2.2–2.5 Å from the nearest H_3O^+ protons.

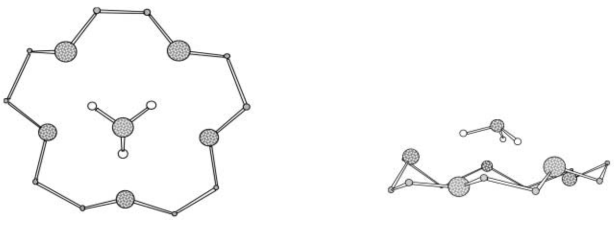

Fig. 5 Optimized structure of the $15c5\cdot H_3O^+$ complex (orthogonal views).

3.2.2 $18c6\cdot H_3O^+$ complex. The calculations were initiated from two different structures of the crown, and, for each of them, two types of coordination modes (denoted by ***a*** and ***b***, see Chart 2), where the H_3O^+ protons respectively form bifurcated (three-center) and linear (two-center) hydrogen bonds. We paid particular attention to the ***b***-type forms, as several papers in the literature point to the "bifurcated" hydrogen bonding patterns in this complex.[26–28] The two conformations of the 18c6 were of D_{3d} symmetry: the "classical" one observed in the complexes with K^+, H_3O^+ and NH_4^+, and the "tennis ball" structure found theoretically by Sun and Kollman.[29] Thus, four starting structures of $18c6\cdot H_3O^+$ were prepared. Their HF/6-31G* optimization led to structures with linear hydrogen bonds only (Fig. 6). The conformer ***1*** (derived from the "classical" D_{3d} structure) is 3.1 kcal mol^{-1} more stable than the conformer ***2***

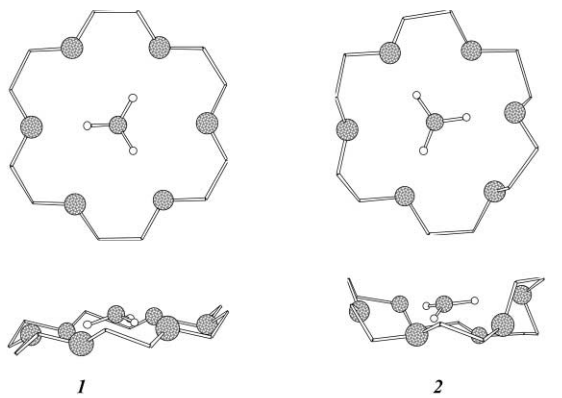

Fig. 6 Optimized structures of the 18c6·H_3O^+ complexes (orthogonal views).

obtained from the "tennis ball" structure. HF/6-31G* optimization initiated from the solid state structure of the 18c6·H_3O^+ complex (*VARKOO*) also led to ***1***, which was verified as a true minimum.

In both the "classical" and "tennis ball" optimized complexes, H_3O^+ forms very short hydrogen bonds, with $H_{H_3O} \cdots O_L$ distances of 1.79 and 1.75 Å, respectively. Note that in the most stable form ***1***, the $O_{H_3O} \cdots O_L$ distances for bonded (2.77 Å) and "non-bonded" (2.87 Å) oxygens of 18C6 are very close, and that the complexed crown is somewhat more planar than the free one: the distance between the two planes of the oxygens "up" and of the oxygens "down" decreases from 0.45 Å in the free state to 0.22 Å in the complex. The oxygen atom of H_3O^+ lies on the C_3 symmetry axis, 0.3 Å above the plane of the "upper" oxygens of 18c6.

In order to find an hypothetical energy minimum with bifurcated hydrogen bonds, we performed 3-21G* calculations on the "classical" conformation of 18c6 imposing a weak constraint (2 kcal mol^{-1}·$Å^2$) at 2 Å on all six $H_{H_3O} \cdots O_L$ distances. The resulting structure is similar to ***1*** but the ligand is more distorted. Reoptimizing this structure using the 6-31G* basis set without any constraint converges again to ***1*** (Fig. 6) where the hydrogen bonds are linear and the ligand is quasi-D_{3d}, as in the solid state structures of 18c6·H_3O^+ complexes.[2]

Basis set effects on the cation binding mode and structural parameters of the 18c6·H_3O^+ complex were also investigated. We thus reoptimized the complex ***1*** using the larger HF/6-31G** and HF/6-311G** basis sets. The resulting distances correspond, within 0.01 Å, to those obtained at the HF/6-31G* level, and the H_3O^+ cation remains slightly pyramidal, forming three linear hydrogen bonds. The $H_{H_3O} \cdots O_L$ distances are identical (1.79 Å) with these three basis sets, and shortest/longest $O_{H_3O^+} \cdots O_L$ distances are 2.77/2.87, 2.75/2.87 and 2.75/2.86 Å with the 6-31G*, 6-31G** and 6-311G** basis sets, respectively. Interestingly, the total Mulliken charge on H_3O^+ (0.85 e) is the same with the three basis sets, and the "bonded"/"non-bonded" oxygen atoms of 18c6 have similar charges (−0.69/−0.66, −0.71/−0.68 and −0.58/−0.53 e with the 6-31G*, 6-31G** and HF/6-311G** basis sets, respectively), which hints at marked attractive interactions between H_3O^+ cation and the two sets of oxygen atoms.

Valence bond MI/6-31G* optimizations starting with linear or bifurcated hydrogen bonds also led to linear $O–H \cdots O_L$ arrangements (Fig. 6). The calculated geometry parameters are slightly different from those found in HF/6-31G* calculations. Thus, the shortest $H_{H_3O} \cdots O_L$ distances are 1.83 Å, whereas the $O_{H_3O} \cdots O_L$ distances are 2.80 and 2.84 Å for "bonded" and "non-bonded" oxygens of the crown-ether, respectively.

Thus, all these calculations confirm that, in the gas phase, H_3O^+ forms three linear hydrogen bonds rather than bifurcated ones with 18c6, and that the crown is of D_{3d}-type symmetry.

3.2.3 Benzo-18-crown-6·H_3O^+ complex. In the optimized B18c6·H_3O^+ complex, the coordination patterns of H_3O^+ are similar to those in 18c6·H_3O^+ (Chart 2 and Fig. 7). The complex displays three linear hydrogen bonds of 1.70–1.74 Å, whereas the other shortest $H \cdots O$ distances vary from 2.44 to 2.51 Å. The anisole oxygen bound to H_3O^+ is more negative (−0.76 e) than the hydrogen bonded ether oxygens (−0.70 e), as a result of larger polarizability of the former.

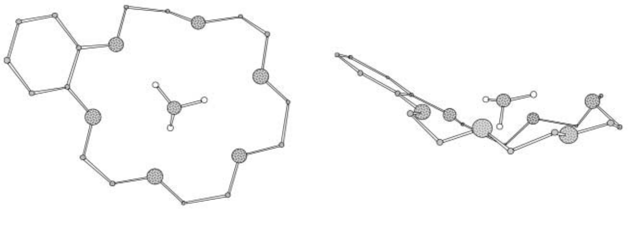

Fig. 7 Optimized structure of the B18c6·H_3O^+ complex (orthogonal views).

3.2.4 PEG-400·$H_5O_2^+$ complex. The initial structure of the complex of $HO–CH_2–(CH_2–O–CH_2)_8–CH_2–OH$ (PEG-400) with $H_5O_2^+$ was prepared by molecular mechanics minimization with the MMFF force field,[30] imposing constraint distances between each terminal $H_5O_2^+$ proton and one oxygen of the ligand. Then, the *ab initio* quantum mechanics optimizations were performed without any constraints.

The first calculation on the PEG·$H_5O_2^+$ complex resulted in dissociation of $H_5O_2^+$ to H_3O^+ and H_2O species. In fact, the $H_5O_2^+ \leftrightarrow H_3O^+ \cdot H_2O$ equilibrium is very sensitive to the environmental effects,[31] and may be shifted by perturbations of its environment. In order to prevent this dissociation, the distances between the central hydrogen and the oxygen atoms were constrained to 1.19 Å, which corresponds to the value obtained by a 6-31G* optimization of $H_5O_2^+$ alone. In the resulting optimized complex, the ligand wraps around the hydrated proton (Fig. 8). Each terminal hydrogen of $H_5O_2^+$ forms one hydrogen bond of 1.95–2.09 Å with one COC or COH oxygen of PEG and interacts more weakly with another one (at 2.2–2.5 Å). Thus, eight of ten oxygen atoms of PEG are involved in the coordination of $H_5O_2^+$.

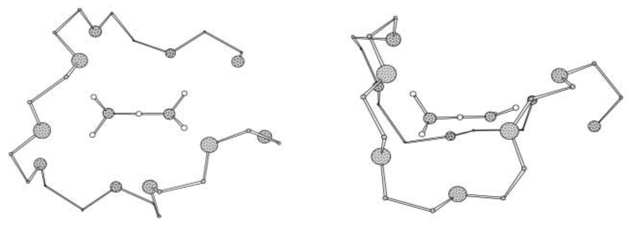

Fig. 8 Optimized structure of the PEG-400·$H_5O_2^+$ complex (orthogonal views).

4 Discussion

4.1 Hydrogen bonding interactions of $H_5O_2^+$ or H_3O^+, as obtained from QM calculations

Gas phase *vs.* solid state structure of the 18c6·H_3O^+ complex. The question arises as to which extent the gas phase calculated structures represent the structure in condensed phases and, particularly, in the studied solutions. To shed light on possible environment (and especially counterion) effects on the structure of the complex itself, we decided to analyze 21 solid state structures of $[H_3O^+ \cdot 18c6]_n An^{n-}$ (where An^{n-} is a counterion, $n = 1, 2$) retrieved from the Cambridge Database.[11] Since the positions of hydrogen atoms were often not well determined, we consider the $O_{H_3O} \cdots O_L$ distances. In the retrieved solid state structures, these distances vary, depending on the system, from 2.55–2.63 Å[26] to 2.81–2.84 Å[23,32–34] or even to 2.89 Å[23] and 2.90–2.94 Å.[35] Such variations might be related to thermal effects, as documented for uncomplexed 18c6, whose bonds appear to be shorter at 300 K than at 100 K.[36] Interestingly, the only structure ($[H_3O^+\cdot 18c6]\ SbCl_6^-$[37]) which has been determined at low temperature (193 K) leads to an excellent agreement between experimental (2.77–2.81 Å) and calculated (2.77–2.87 Å) distances. One could also try to attribute the lengthening of $O_{H_3O} \cdots O_L$ distances to increased cation–anion interactions which thus compete with the cation–crown interactions. This is not the case. Indeed, in the structures containing AsF_6^-, I_7^-, BF_4^- as counter-ions, the O_{H_3O} atom is nearly equidistant (2.68–2.73 Å) from the six ether oxygens,[38,39] whereas in the structure containing the more bulky hexa-molybdate anion the $O_{H_3O} \cdots O_L$ distances vary from 2.70 to 2.82 Å. The distances calculated in the gas phase (2.77–2.87 Å) are within the range of values obtained in crystals, therefore suggesting that environment and counterion effects, if any, are weak. This is not surprising as the complexed H_3O^+ cation can hardly bind to anions (they would be repulsed by its oxygen atom), or to cations (repulsed by the +1 charge), therefore displaying hydrophobic behaviour. On the computational side, it was also shown that the structures of complexes of macrocyclic and open-chain ligands simulated in a weakly polar solvent like chloroform are similar to those modeled in the gas phase.[40] Therefore, the reported quantum mechanically optimized structures of H_3O^+ or $H_5O_2^+$ complexes should be close to those in DCE solution.

Hydrogen bonds in II, IV–VI complexes. Quantum mechanics calculations show that in the $\mathbf{L}\cdot(H^+\cdot nH_2O)$ complexes, some oxygens of **L** form short linear or pseudo-linear (150–180°) $OH \cdots O_L$ hydrogen bonds with the hydrated proton, whereas other oxygens of **L** experience secondary electrostatic interactions. It should be noted that the strength of individual hydrogen bonding interactions, as reflected by the $OH \cdots O_L$ distances, does not simply relate to the total binding energy ΔE of the hydrated proton, which results from all contributions, including those of "non-bonded" oxygens. According to the HF/6-31G* calculations, the H_3O^+–**L** attraction energy ΔE is highest in the 18c6 complex (103.8 kcal mol^{-1}), and further decreases from B18c6 (93.0 kcal mol^{-1}) to 15c5 (85.5 kcal mol^{-1}) 1 : 1 complexes, due to the poorer fit between the cation and the host cavity. The H_3O^+ oxygen is more remote from the average macrocyclic plane of 15c5 (1.36 Å) than of B18c6 (0.65 Å) or 18c6 (0.22 Å), thus indicating that H_3O^+ is least shielded and most accessible to other external coordinating species in $15c5\cdot H_3O^+$. This may explain why this complex transforms into $2(15c5)\cdot H_5O_2^+$ in the excess of the ligand, whereas $18c6\cdot H_3O^+$ and $B18c6\cdot H_3O^+$ complexes are stable at all studied concentrations of the ligands. We also note that a solid state structure has been reported for $2(15c5)\cdot H_5O_2^+$,[2] but not, to our knowledge, for $15c5\cdot H_3O^+$.

4.2 IR spectra of $H_5O_2^+$ in the complexes

The IR studies show that in the **I–III** complexes, $H_5O_2^+$ coordinates to four oxygens (O_S), which belong to water or to the ligand (O_L). The spectra of the symmetrical $H_5O_2^+\cdot 4O_S$ cation contain three intense bands: the $\nu_{as}(OHO)$ band at 900–1100 cm^{-1} of the central O–H^+–O group, the "out of plane" bending $\delta(HOH)$ band at 1720–1740 cm^{-1} of the four peripheral OH groups, and stretching $\nu_s(OH)$ and $\nu_{as}(OH)$ bands at 2900–3200 cm^{-1} of the $O\text{–}H \cdots O_S$ bonds. There is also an extended continuous absorption in the 3000–920 cm^{-1} region due to the vibrations of $O\text{–}H \cdots O_W$ groups. In the absence of polyether ligand, we characterize the $[H_5O_2^+\cdot 4H_2O]$ species (**I**), whose IR spectrum is reported, to our knowledge, for the first time in an aprotic solvent. Compared to the spectra reported for the $[H_5O_2^+(OH_2\cdot 2O_S)_2L_2]$ species[7,9,10] it differs mostly by the absorption bands of H_2O molecules: the corresponding frequencies and half-widths of $\delta(H_2O)$ and $\nu(OH)$ bands in **I** are typical for OH groups hydrogen bonded to oxygen atoms (Fig. 1e). Substitution of the four H_2O of **I** by COC groups of a polyether, (*i.e.* when passing from complexes **I** to **II** or **IV**), leads to expected changes in the spectrum of $H_5O_2^+$: the band $\delta(HOH)$ at 1738 cm^{-1}, which is most sensitive to the coordination of H_2O molecules to $H_5O_2^+$, becomes narrower, and the intensity of the background continuum decreases (Fig. 2c, e).

4.3 "Extra" water in the DCE solution

The presence of self-associated water molecules not bound to the hydrated proton (referred to as "extra water") is a specific feature of water-saturated DCE solutions of polyethers and their complexes **I–VI**. Presumably, "extra water" forms the core of reverse nano-micelles which are often generated in water saturated organic solutions.[7–9]

In the absence of proton complexes, the content of "extra water" in DCE solutions has been found to be markedly dependent on the nature of the polyether: such water was "dragged" by even small quantities of free PEG, but not by the weaker surfactants 15c5, 18c6 and B18c6. This contrasts with the presence of hydrated proton complexes **I–VI** which always solubilize "extra" water in DCE solutions. Generally, this water content decreases when the concentration of the complexes increases, which is typical for salting-out effects. This suggests that the interactions between "extra" water and **I–VI** complexes are weak. On the other hand, the addition of a small excess of crown-ether to the solutions of **III–VI** complexes leads to the decrease or disappearance of "extra" water absorption in the IR spectra. This can be explained if one assumes that crown-ethers display outer-sphere coordination to these complexes, thus shielding them from nano-micelles, and leading to some destabilisation of the latter.

It should be noted that the concentration of "extra" water may significantly exceed the solubility of water in DCE. Therefore, formation of water-containing nano-micelles should be taken into account when studying hydration effects and the composition of the complexes in extraction systems.

Conclusions

Based on IR spectroscopy and quantum mechanics studies, we characterize the complexes formed by the hydrated proton (H_3O^+ or $H_5O_2^+$) with polyethers (**L** = 15-crown-5, 18-crown-6, benzo-18-crown-6 and polyethylene glycols PEG-400 and PEG-600) in 1,2-dichloroethane solution saturated with water. It has been shown that the state of the hydrated proton and composition of the complexes vary as a function of the nature and relative concentration of **L**. Thus, 15-crown-5 forms $\mathbf{L}\cdot H_3O^+$ and $2\mathbf{L}\cdot H_5O_2^+$ complexes at small and high concentrations of **L**, respectively. 18-Crown-6 and benzo-18-crown-6 form 1 : 1 complexes with H_3O^+ at all studied concentrations, while polyethylene glycols form 1 : 1 complexes with $H_5O_2^+$. According to the QM results, the hydrated proton forms, as much as possible, linear (two-center), rather than bifurcated (three-center) hydrogen bonds with the oxygen atoms of the polyether ligand. This is also supported by a recent CP-MD study on the $18c6\cdot H_3O^+$ complex.[41] Hydrogen bonds are calculated to be stronger in 1 : 1 complexes with crown-ethers than with polyethylene glycol. However, beyond static features of the complexes, the dynamic ones, including possible quantum effects, remain to be characterized.

A particularly interesting change in the proton state is observed with 15c5, which evolves from $15c5\cdot H_3O^+$ to $2(15c5)\cdot H_5O_2^+$ complexes as the ligand concentration is increased. This contrasts with 18c6 and B18c6 which complex one H_3O^+ species only at different concentrations of the ligand. This phenomenon is explained by the smaller cation–ligand interaction energy and larger accessibility of H_3O^+ in 15c5·H_3O^+, compared to the other complexes.

We also report the first IR characterization of the $[H_5O_2^+\cdot 4H_2O]$ cation in an "inert" solvent, which is compared to the $[H_5O_2^+(OH_2\cdot 2O_L)_4]$ species.

Finally, it has been shown that the water saturated DCE solutions of hydrated proton complexes **I–VI** additionally contain self-associated water. This "extra water" likely aggregates, forming structures like reversed nano-micelles which weakly (extra-spherically) interact with dissolved complexes. Such "extra water" complicates the analysis of complexation or liquid–liquid extraction data, but has to be taken into account to correctly depict the nature of the complexes in solution.

Acknowledgements

This work was supported by the INCO-COPERNICUS grant (project ERB IC15-CT98-0208). The authors thank E. Kochanski and A. Dedieu for fruitful discussions. ES gratefully acknowledges GW for invitation as Professor at Strasbourg University in 2000.

References

1 R. B. Sharma and P. Kebarle, *J. Am. Chem. Soc.*, 1984, **106**, 3913.
2 P. C. Junk, *Rev. Inorg. Chem.*, 2001, **21**, 93 and references cited therein.
3 H. Hassaballa, J. W. Steed, P. C. Junk and M. R. J. Elsegood, *Inorg. Chem.*, 1998, **37**, 4666.
4 P. C. Junk and J. L. Atwood, *J. Chem. Soc., Chem. Commun.*, 1995, 1551.
5 J. van Eerden, M. Skowronska-Plasinska, P. D. J. Grootenhuis, S. Harkema and D. N. Reinhoudt, *J. Am. Chem. Soc.*, 1989, **111**, 700.
6 E. S. Stoyanov, *Zh. Struct. Khim. (Russ.)*, 1993, **34**, 72.
7 E. S. Stoyanov, *J. Chem. Soc., Faraday Trans.*, 1997, **93**, 4165.
8 E. S. Stoyanov and V. N. Kolomiichuk, *Mendeleev Commun.*, 1997, 180.
9 E. Stoyanov, *J. Chem. Soc., Faraday Trans.*, 1998, **94**, 2803.
10 E. S. Stoyanov, *Phys. Chem. Chem. Phys.*, 1999, **1**, 2961.
11 F. H. Allen and O. Kennard, *Chem. Des. Autom. News*, 1993, **8**, 31.
12 *Cambridge Structural Database*, 2000.
13 SPARTAN5.0, Wavefunction Inc., Irvine, USA, 1997.
14 E. Gianinetti, I. Vandoni, A. Famulari and M. Raimondi, *Adv. Quantum Chem.*, 1998, **31**, 251.
15 M. W. Schmidt, K. K. Baldridge, J. A. Boatz, S. T. Elbert, M. S. Gordon, J. Jensen, S. Koseki, N. Matsunaga, K. A. Nguyen, S. J. Su, T. L. Windus, M. Dupuis and J. A. Montgomery, *J. Comput. Chem.*, 1993, **14**, 1347.
16 F. B. van-Duijneveldt, J. G. C. M. van-Duijneveldt-van-de-Rijdt and J. H. van-Lenthe, *Chem. Rev.*, 1994, **94**, 1873.
17 A. Famulari, F. Moroni, M. Sironi, E. Gianinetti and M. Raimondi, *J. Mol. Struct. (THEOCHEM)*, 2000, **259**, 209.
18 A. Famulari, F. Moroni, M. Sironi and M. Raimondi, *J. Comput. Chem.*, 2000, **24**, 341.
19 F. Moroni, A. Famulari and M. Raimondi, *J. Phys. Chem. A*, 2001, **105**, 1169.
20 J. Sponer, J. Leszczynski and P. Hobza, *J. Phys. Chem.*, 1996, **100**, 1965.
21 N. U. Zhanpeisov and J. Leszczynski, *J. Phys. Chem.*, 1998, **102**, 6167.
22 J. E. D. Bene and M. J. T. Jordan, *J. Mol. Struct. (THEOCHEM)*, 2001, **573**, 11.
23 R. Chênevert, D. Chamberland, M. Simard and M. Brisse, *Can. J. Chem.*, 1990, **68**, 797.
24 R. Chênevert, A. Rodrigue, M. Pigeon-Gosselin and R. Savoie, *Can. J. Chem.*, 1982, **60**, 853.
25 R. Chênevert, A. Rodrigue, P. Beauchesne and R. Savoie, *Can. J. Chem.*, 1984, **62**, 2293.
26 J. L. Atwood, S. G. Bott, P. C. Junk and M. T. May, *J. Organomet. Chem.*, 1995, **487**, 7.
27 J. L. Atwood, S. G. Bott, P. C. Junk and M. T. May, *J. Coord. Chem.*, 1996, **37**, 89.
28 M. Calleja, K. Johnson, W. J. Belcher and J. W. Steed, *Inorg. Chem.*, 2001, **40**, 4978.
29 Y. Sun and P. A. Kollman, *J. Comput. Chem.*, 1992, **13**, 33.
30 T. A. Halgren, *J. Comput. Chem.*, 1996, **17**, 490.
31 J. C. Jiang, Y.-S. Wang, H.-C. Chang, S. H. Lin, Y. T. Lee, G. Niedner-Schatteburg and H.-C. Chang, *J. Am. Chem. Soc.*, 2000, **122**, 1398.
32 J.-P. Behr, P. Dumas and D. Moras, *J. Am. Chem. Soc.*, 1982, **104**, 4540.
33 R. Chênevert, D. Chamberland, M. Simard and F. Brisse, *Can. J. Chem.*, 1989, **67**, 32.
34 J. L. Atwood, S. G. Bott, A. W. Coleman, K. D. Robinson, S. B. Whetstone and C. M. Means, *J. Am. Chem. Soc.*, 1987, **109**, 8100.
35 B. M. Bulichev and V. K. Belsky, *Coord. Khim. (Russ.)*, 1995, **40**, 1834.
36 P. Maverick, P. Seiler, B. Schweitzer and J. D. Dunitz, *Acta Crystallogr., Sect. B*, 1980, **36**, 615.
37 C. B. Shoemaker, L. V. McAfee, D. P. Shoemaker and C. W. DeKock, *Acta Crystallogr., Sect. C*, 1986, **42**, 1310.
38 H. Feinberg, I. Columbus, S. Cohen, M. Rabinovitz, V. Selig and G. Shoham, *Polyhedron*, 1993, **12**, 2913.
39 P. C. Junk, L. R. MacGillivray, M. T. May, K. D. Robinson and J. L. Atwood, *Inorg. Chem.*, 1995, **34**, 5395.
40 A. Varnek, C. Sirlin and G. Wipff, in *Crystallography of Supramolecular Compounds*; ed. G. Tsoucaris, Kluwer, Dordrecht, 1996; p. 67.
41 M. Buehl and G. Wipff, *J. Am. Chem. Soc.*, 2002, in the press.